

Predicting the thermal conductivity of polymer composites with one-dimensional oriented fillers using the combination of deep learning and ensemble learning

Yinzhou Liu ^{a,b}, Weidong Zheng ^b, Haoqiang Ai ^b, Lin Cheng ^b, Ruiqiang Guo ^b, Xiaohan Song ^{b,*}

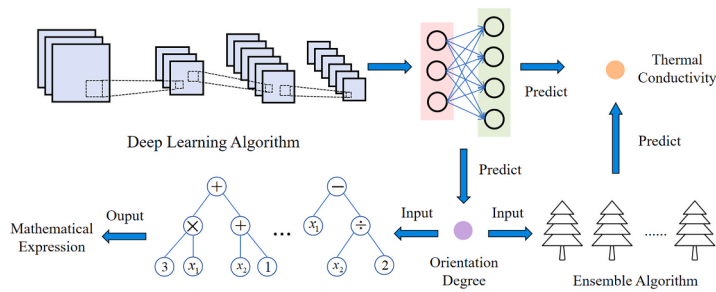
^a Institute of Advanced Technology, Shandong University, Jinan 250061, PR China

^b Shandong Institute of Advanced Technology, Jinan 250100, PR China

HIGHLIGHTS

- Deep learning (CNN) and ensemble learning (RFR) was successfully used to accurately predict the thermal conductivity of polymer composites with one-dimensional oriented fillers.
- Introduced a new descriptor, "Orientation degree (O_d)," to quantitatively describe the spatial distribution of one-dimensional fillers, significantly enhancing prediction accuracy.
- The mathematical expressions between the different descriptors and the thermal conductivity of the composite were obtained by using the symbolic regression algorithm.
- The proposed method reduces the need for extensive retraining of models, offering a practical solution for material property prediction in advanced materials design and energy efficiency applications.

GRAPHICAL ABSTRACT



ARTICLE INFO

Keywords:
Deep learning
Ensemble learning
Thermal conductivity
Orientation degree
Polymer composites

ABSTRACT

Polymer composites with one-dimensional (1D) oriented fillers, recognized for their high thermal conductivity (TC), are extensively utilized in cooling electronic components. However, the prediction of the TC of composites with 1D oriented fillers poses a challenge due to the significant impact of filler orientation on composite TC. In this paper, we use a strategy that combines deep learning and ensemble learning to efficiently and quickly predict the TC of composites with 1D oriented fillers. First, as a control, we used convolutional neural network (CNN) model to predict the TC of 1D carbon fiber-epoxy composite, and the R-squared (R^2) on the test set reached 0.924. However, for composites consist of different matrices and fillers, the CNN model needs to be retrained, which greatly wastes computing resources. Therefore, we define a descriptor 'Orientation degree (O_d)' to quantitatively describe the spatial distribution of the 1D fillers. CNN model was used to predict this structural parameter, the accuracy R^2 can reach 0.950 on the test set. Using O_d as a feature, random forest regression (RFR)

* Corresponding author.

E-mail address: xiaohan.song@iat.cn (X. Song).

was used to predict the TC, and the accuracy R^2 reached 0.954 on the test set, which was higher than that of CNN control group. We further successfully extended this strategy to composites consist of different 1D fillers and matrices, and only one CNN model and one RFR model needed to be trained to achieve fast and accurate TC prediction. This strategy provides valuable insights and guidance for machine learning-based material property prediction.

1. Introduction

As the size of electronic components continues to shrink and their integration complexity increases, the thermal flux density they generate has significantly risen. This trend underscores the urgent need for efficient thermal interface materials (TIMs) that can effectively manage the cooling of these components [1–3]. Traditional thermal interface materials (TIMs) are typically composed of high thermal conductivity (TC) particulate fillers and low electrical conductivity polymer matrices. While these materials are relatively easy to prepare, their TC is generally low, only achieving high levels when the filler loading is significantly high [4–6]. In certain applications, we often desire TIMs to exhibit high TC in a specific direction. For example, in chip cooling, it is preferable for TIMs to have high TC perpendicular to the chip surface to enhance heat dissipation. Some one-dimensional (1D) materials, such as carbon fibers and carbon nanotubes, have much higher TC along their axial direction compared to their radial direction [7,8]. If these materials can be appropriately aligned within the matrix, a high TC can be achieved with only a small volume fraction of the fillers. Besides, when using high-density electronic design software, the ability to quickly and accurately predict the thermal conductivity of composites with 1D oriented fillers plays a key role in selecting suitable TIMs for efficient thermal management. Therefore, studying polymer composites with 1D oriented fillers is essential for optimizing heat dissipation and ensuring the reliability of high-density electronic components [9–14].

There are many factors that influence the TC of 1D composites, such as the TC of the filler, the TC of the matrix, and the interactions between the filler and the matrix [15,16]. However, a key factor is the spatial orientation of the 1D fillers. Nan et al. [17] proposed a series of effective medium theories (EMT) based on multiple scattering methods to predict the impact of filler geometry and spatial orientation on the TC of composites. These theories extend the applicability of traditional effective medium theories. Fu et al. [18] studied the effects of carbon fiber orientation and length on composite TC using a laminated analogy method (LAM). They also employed the concept of an equivalent matrix to account for the interactions between carbon fibers. Yang et al. [19] proposed a new analytical method based on unit cell modeling and EMT to predict the TC of 1D composites in different directions. Although these methods enable rapid prediction of thermal conductivity, they require significant simplifications of real-world conditions, which can result in some loss of accuracy. Common methods for obtaining the TC of composites also include finite element method (FEM), and finite volume method (FVM) [20–23]. The FEM and FVM solve differential equations through numerical calculations to determine the TC of composites. Compared with empirical formulas, although they are more accurate, they require more time cost and computing resources. Therefore, finding a method that can quickly and accurately predict the TC of carbon fiber composites is particularly important.

In recent years, the emergence of machine learning methods has opened up new possibilities for achieving the aforementioned goals [24–30]. Among these methods, convolutional neural network (CNN) is widely used in image recognition and processing, and stand out as powerful tools in the field of deep learning. For instance, Han et al. [31] employed CNN to predict the TC of two-dimensional porous materials, comparing their results with empirical formulas to validate the accuracy of deep learning algorithms. Rong et al. [32] used CNN to predict the TC of three-dimensional particulate composite materials from two-dimensional cross-sectional images, and explored the effect of the

number and size of these cross-sectional slices on the model's precision. CNN possess the capability to automatically learn features from microstructure images of composite materials, so it can effectively obtain the directional arrangement degree of 1D fillers and the TC of composite materials [33]. But deep learning often takes a lot of time and computing resources. Ensemble learning, such as random forest regression (RFR), can improve the generalization and accuracy of the model by combining multiple different learning periods, and requires less time and computational resources. Compared with only using deep learning, the combination of deep learning and ensemble learning, specifically, obtains the microstructure features of materials through deep learning, and then associates the obtained structural features with the properties of materials through ensemble learning, can effectively accelerate the training process and improve the prediction accuracy. And the symbolic regression can enhance interpretability.

In this study, based on the combination of deep learning and ensemble learning mentioned above, we successfully achieved millisecond-level predictions of the TC of composites containing 1D oriented fillers while maintaining accuracy. Firstly, taking 1D carbon fiber-epoxy resin composites as an example, CNN models were developed using the internal cross-sections and external surfaces of the Representative Volume Element (RVE) models as input data respectively. It was found that using the external surfaces as input could achieve more accurate prediction of the TC of the composite. However, multiple CNN models need to be trained for different fillers and matrices, which consumes a lot of time and computing resources. Therefore, we defined the "Orientation degree (O_d)" parameter to describe the spatial distribution of 1D fillers. CNN model was used to predict O_d , and O_d was then used as a descriptor to train RFR model for predicting TC of composites. This strategy has been successfully applied to 1D carbon fiber-epoxy composites. Subsequently, we extended this strategy to composites with different 1D fillers and matrices, and the accuracy R^2 reached 0.960 on the test set. In addition, we used symbolic regression (SR) to derive a mathematical expression of the composites TC, which enhances the interpretability.

2. Methods

2.1. Microstructure

The RVE method is widely employed in the modeling of various materials due to its high computational accuracy and low computational cost [19,34,35]. In this paper, we utilize the commercial software MATLAB and COMSOL for large-scale and rapid modeling of carbon fiber composites. By leveraging the programming capabilities of MATLAB, we have managed to highly automate the complex modeling process, thereby saving a considerable amount of time. Before initiating the modeling process, we employed a sample enlargement method (SEM) to determine the appropriate size of the RVE [36,37], as illustrated in Fig. 1. Due to the randomness inherent in the modeling, multiple model sets were generated under the same size, and the average of the computed results was taken to represent the outcome for that particular size. When the calculation results start to stabilize with changes in size, the corresponding RVE size can be determined. The relevant calculation formula is as follows:

$$\frac{T_x^{i+1} - T_x^i}{T_x^i} < Tol = 5\% \quad (1)$$

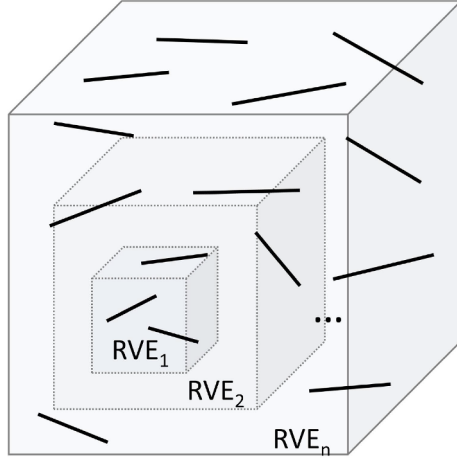


Fig. 1. Sample enlargement method.

where T_x is the average TC along the x-axis for a given size, i is the RVE model at the i th size, and Tol is the tolerance for stagnation. This approach balances the need for accurate representation of the material's behavior with computational efficiency, ensuring that the selected RVE size is both representative of the material's properties and manageable for simulation purposes.

During the modeling phase, we employed the Random Sequential Addition (RSA) algorithm to construct the carbon fibers [21,38,39]. This algorithm not only offers flexible control over randomness but also prevents intersections between carbon fibers, resulting in a model that more closely aligns with real-world scenarios. We set the diameter of carbon fibers to $1.5 \mu\text{m}$, the volume fraction (Vol) of carbon fibers in the range of 1–10, and their aspect ratio (L/D) also between 1 and 10, where L represents the length of the carbon fiber and D denotes its diameter. The minimum distance between fillers is set to $0.5 \mu\text{m}$. The angle (θ) between the carbon fibers and the x-axis was set within $5\text{--}50^\circ$, as illustrated in Fig. 2. For instance, when the angle θ is set to 20° , the distribution of carbon fibers adheres to a normal distribution, characterized by a mean of 0 and a standard deviation of 20, with φ assuming values within the range of 0 to 360° . Consequently, most of the fiber angles will fall within the conical angle shown in Fig. 2. The detailed parameters are listed in Table 1.

Table 1
Parameters of modeling.

Parameters	Range	Uniform Distribution Interval
Vol (%)	1–10	1
D/L	1–10	1
θ ($^\circ$)	5–50	5

2.2. TC calculation

2.2.1. Calculation method

During the computation, we focused solely on the conductive heat transfer in solids, disregarding convective and radiative heat exchange. The governing equation for a steady state with no internal heat sources is:

$$\nabla^2 T = \frac{\partial^2 T}{\partial x^2} + \frac{\partial^2 T}{\partial y^2} + \frac{\partial^2 T}{\partial z^2} \quad (2)$$

where T is the temperature, the unit is K.

Given that our subject of study is carbon fiber composite materials with a degree of orientation, our interest primarily lies in the TC along the x-axis. Here, we employed Fourier's law of heat conduction for our calculations:

$$q_x = -\lambda \frac{\partial T}{\partial x} \quad (3)$$

where q_x is the heat flux density along x-axis, $\frac{\partial T}{\partial x}$ is the temperature gradient along the x-axis, and λ is the conductivity of the material.

Given the notable anisotropic TC of carbon fibers, their TC is typically expressed in the form of a tensor:

$$\lambda = \begin{pmatrix} \lambda_{xx} & 0 & 0 \\ 0 & \lambda_{yy} & 0 \\ 0 & 0 & \lambda_{zz} \end{pmatrix} \quad (4)$$

when $\lambda_{xx} = \lambda_{yy} = \lambda_{zz}$, it denotes isotropic TC.

Due to the adoption of the FEM by COMSOL software for calculating the TC of solids, this approach involves dividing a large solid domain into numerous smaller, finite sub-domains. This process is known as discretization or mesh division, as illustrated in Fig. 3. Consequently, the heat flux density along the x-axis of the RVE model can be represented as the average of the heat flux densities along the x-axis for each sub-domain:

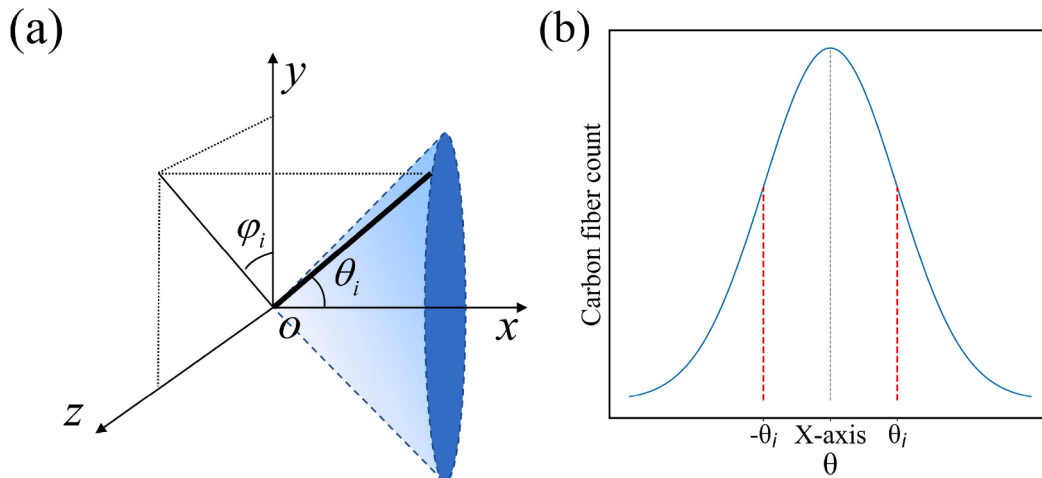


Fig. 2. (a) Definition of carbon fiber orientation angle. (b) Schematic diagram of the normal distribution of carbon fibers .

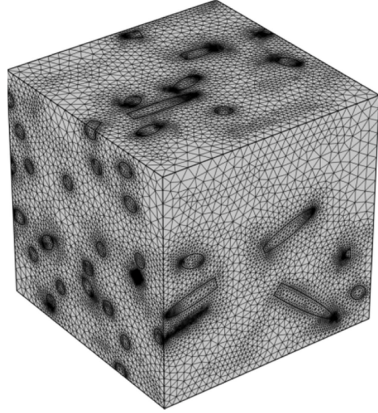


Fig. 3. Mesh division.

$$q_x = \frac{1}{N} \sum_{i=1}^N q_x^i \quad (5)$$

where N is the number of mesh elements, and q_x^i is the heat flux density along the x -axis for the i th mesh element.

2.2.2. Boundary conditions

To better simulate the real-world operating conditions of electronic components, we have reasonably established the boundary conditions for the model. As illustrated in Fig. 4, we set the temperature of the high-temperature surface (the right surface) as $T_r = 343.15 K$ to simulate the high-temperature environment that may be generated during the operation of electronic devices. The temperature of the low-temperature surface (the left surface) was set as $T_l = 303.15 K$, which to mimic the ambient environmental temperature. Furthermore, to reflect the reality that certain surfaces in electronic components may not directly engage in heat exchange, we set the remaining four walls of our model as adiabatic surfaces. Hence, the boundary conditions can be given by the following expression:

$$\begin{cases} T_r = 343.15K; T_l = 303.15K \\ \left. \frac{\partial T}{\partial n} \right|_{\Gamma} = 0 \end{cases} \quad (6)$$

where Γ refers to the four adiabatic surfaces, n is the normal vector of the adiabatic surface.

2.2.3. Set TC of materials

The matrix of the composites material we chose is epoxy resin, which is widely used in thermal interface materials. Epoxy resin exhibits

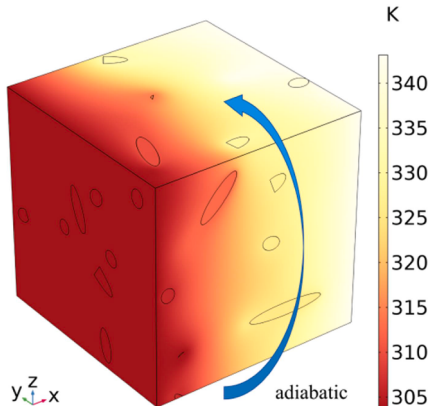


Fig. 4. Boundary conditions.

isotropic TC, meaning it can uniformly transfer heat in all directions. Herein, we assigned the TC of epoxy resin as $\lambda^2 = 0.2 W/mK$ [40].

The filler carbon fiber we selected is a typical example of 1D materials, renowned for their markedly anisotropic thermal conductive properties. This anisotropy is characterized by a significantly higher TC along the fibers' axial direction compared to their radial direction [41]. To simplify the computational model without losing the essence of this anisotropic behaviour, we focus exclusively on the axial TC of the carbon fibers. We have assigned a value of $\lambda^1 = 500 W/mK$ for this axial TC [42], which is a realistic representation for many types of carbon fibers.

In accordance with the angles and coordinate system defined in Fig. 2, we project the axial TC coefficient onto the three principal axes of the coordinate system. Considering the inherent uncertainty in the arrangement of carbon fibers within the composite material, this projection is vital for accurately simulating the conduction of heat through the carbon fibers in various directions. The anisotropic TC of the carbon fibers can be represented as follows:

$$\begin{cases} \lambda_{xx}^1 = \lambda^1 \cos\theta \\ \lambda_{yy}^1 = \lambda^1 \sin\theta \cos\phi \\ \lambda_{zz}^1 = \lambda^1 \sin\theta \sin\phi \end{cases} \quad (7)$$

2.3. Build the datasets

In this study, we utilized two-dimensional images as the primary data source for CNN, which is particularly pertinent when dealing with three-dimensional materials. By selecting appropriate two-dimensional cross-sections, it is possible to effectively represent their three-dimensional structures, which has been validated by various scholars [43–45]. We developed a dataset based on the internal cross-sections of the model, which we refer to as dataset_A. As illustrated in Fig. 5(a), we uniformly selected 9 sections perpendicular to the x -axis, y -axis, and z -axis respectively, resulting in a total of 27 cross-sectional images for each sample.

Due to the use of polymer materials as the matrix in thermal interface materials, their inherent transparency allows us to observe the internal structure of the materials. Zhang et al. [46] has demonstrated the capability of CNN to reconstruct the entire three-dimensional structure of an object from its external surface. Therefore, we constructed dataset_B using the 6 external surfaces of the RVE models, as illustrated in Fig. 5(b). The transparency of the matrix allows these external surfaces to be perceived as projections of the carbon fiber along certain directions, effectively encapsulating the volumetric structural information to a great extent. The samples used in dataset_A and B are all derived from the 1000 RVE models we constructed, so both datasets_A and B have 1000 samples.

2.4. CNN model

Currently, CNN are primarily utilized for image recognition tasks [47,48], but some researchers have also adapted them for regression prediction tasks [31,32]. Within CNN, the most common and critical hidden layers include convolutional layers, pooling layers, and fully connected layers. The convolutional layers are designed for extracting features from images, while pooling layers reduce the size of the feature maps to conserve computational resources. The fully connected layers integrate all preceding information for final prediction. To achieve non-linearity in neural networks, activation functions are typically included in hidden layers. To prevent issues like gradient explosion or vanishing during training, each hidden layer usually contains a Batch Normalization (BN) layer [49]. Additionally, to avoid overfitting, strategies such as controlling the depth or width of the neural network or employing dropout techniques are commonly adopted [50].

In this study, the neural network architecture we employed is illustrated in Fig. 6. We configured the input layer to have a dimension of

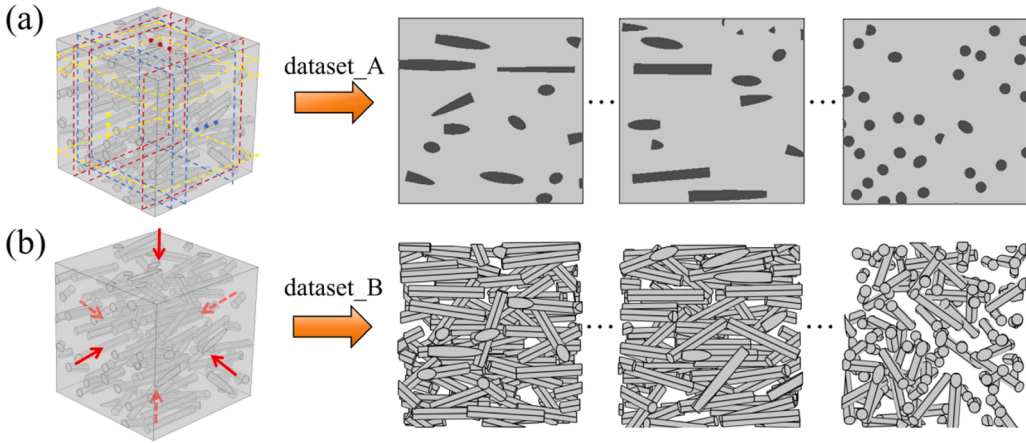


Fig. 5. The (a) internal cross-sections and (b) external surfaces of the RVE models are selected as dataset_A and dataset_B, respectively.

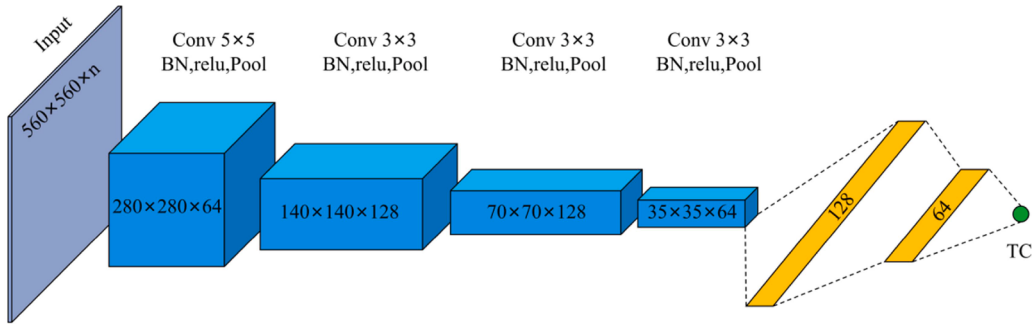


Fig. 6. CNN model architecture diagram.

560×560 . Moreover, for the input layer, 'n' is determined by the number of images contained within the input samples. Specifically, 'n' is set to 6 when the input data consist of the external surfaces of the RVE, and it increases to 27 for the internal cross-sections of the RVE. Additionally, our model comprises four convolutional layers and two fully connected layers. The first convolutional layer has a kernel size of 5×5 , while the remaining three convolutional layers have a kernel size of 3×3 . To prevent gradient explosion during training, a BN layer is incorporated after each convolutional layer. Furthermore, each convolutional layer utilizes the relu activation function, accompanied by a MaxPool layer with a size of 2×2 and a stride of 2. The two fully connected layers contain 128 and 64 neurons, respectively. Throughout the training process, we employed the Mean Square Error (MSE) as the loss function and used Root Mean Square Error (RMSE) and R-squared (R^2) as evaluation metrics. The expressions for these are as follows:

$$MSE = \frac{1}{N} \sum_{i=1}^N (y_i - \hat{y}_i)^2 \quad (8)$$

$$RMSE = \sqrt{\frac{1}{N} \sum_{i=1}^N (y_i - \hat{y}_i)^2} \quad (9)$$

$$R^2 = 1 - \frac{\sum_{i=1}^n (y_i - \hat{y}_i)^2}{\sum_{i=1}^n (y_i - \bar{y})^2} \quad (10)$$

where N is the number of samples, y_i is the true value of the i th sample, \hat{y}_i is the predicted value of the i th sample, \bar{y} is the average of the true values of all samples.

2.5. SR algorithm

SR algorithm is a machine learning technique aimed at discovering mathematical expressions between given input and output data. The algorithm typically relies on genetic algorithms to search for the best expressions, as illustrated in Fig. 7. Initially, the algorithm randomly generates some individuals, often in the form of tree structures, where internal nodes consist of operators and external nodes consist of variables or constants. Subsequently, through an appropriate evaluation function, individuals with the highest fitness are selected as parents for genetic operations such as crossover and mutation. Poor-performing individuals are eliminated after each iteration until the evolution terminates or a specified number of iterations is reached, resulting in the final mathematical expression. Due to the excellent interpretability of mathematical expressions, this algorithm has been widely applied in materials research [51–53]. In this study, the SR algorithm was employed to derive mathematical expressions of the TC of composite materials.

3. Results

3.1. RVE size determination and TC calculation by FEM

We determined the size of RVE before commencing the large-scale datasets construction. Taking the case of randomly distributed carbon fibers as an example, we conducted observations using SEM. For each RVE size, we randomly generated five models and used their average values to assess stability. In these models, the diameter, L/D and Vol of the carbon fibers was set to $3 \mu\text{m}$, 10, and 5 %, respectively. As evident from Fig. 8, the TC of the models began to stabilize when the RVE size reached 50 micrometers, meeting the requirements of Eq. (1). Therefore, to minimize the computational expenses, we finally chose 50

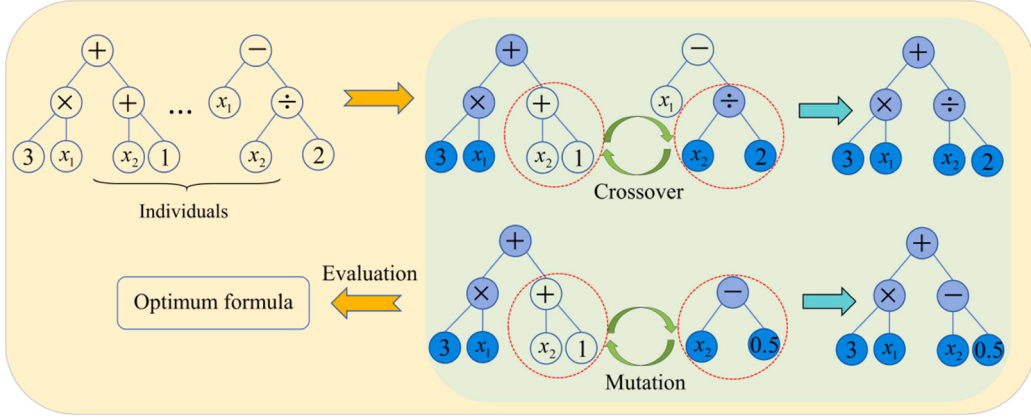


Fig. 7. SR algorithm flowchart.

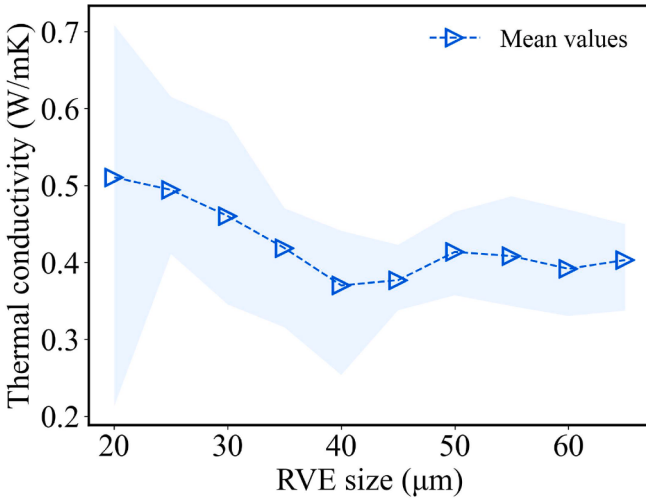


Fig. 8. TC versus RVE size.

micrometers as the RVE size.

After determining the size of RVE, we constructed 1000 RVE models within the parameter ranges specified in Table 1 and calculated their respective thermal conductivities. We plotted the data distribution within the various parameter ranges based on this dataset as shown in Fig. 9 (a-c). It can be seen that an increase in volume fraction of carbon fibers significantly enhances the TC of the composites across different aspect ratios. Additionally, at the same volume fraction, the TC of the composites also increases with the aspect ratio. This is because a higher

aspect ratio implies longer carbon fibers, which help form more effective thermal conduction paths, thereby improving the overall TC. However, the impact of the carbon fiber angles on the TC of the composites is more complex. When the aspect ratio is low, the shape of the carbon fibers tends to be isotropic, and the effect of the normally distributed angles on the TC is not very pronounced. As the aspect ratio increases, the anisotropic effect becomes more apparent. In this case, smaller angles (e.g., $\theta=10^\circ$) correspond to higher TC, while larger angles (e.g., $\theta=50^\circ$) correspond to lower TC. Smaller angles mean that the carbon fibers are more orderly aligned and more parallel to the heat flow direction, which facilitates heat conduction along the carbon fibers, resulting in higher TC. Conversely, larger angles imply a more disordered arrangement of carbon fibers within the matrix, increasing the scattering and obstruction in the thermal conduction path, thus reducing TC.

3.2. Prediction of TC based on CNN

During the training process, we randomly divided the datasets into a training set and a test set in a 9:1 ratio. Random splitting of datasets is beneficial to model outcomes because it ensures diversity and representativeness of the training and testing sets, thereby improving the performance of the model and reliability of the evaluation. Initially, we focused on exploring the impact of the number of cross-sectional images in dataset_A on the performance of the CNN model. Given that carbon fibers are distributed in three-dimensional space, and determining their angles in this space requires at least two cross-sectional images from different directions, it's essential, as shown in Fig. 2, that one of these sections be perpendicular to the x-axis. Here, we started by using the 9 sections perpendicular to the x-axis as the input data, then progressively incorporated the 9 sections perpendicular to the z-axis and finally the 9 sections perpendicular to the y-axis, to observe the effect on the model.

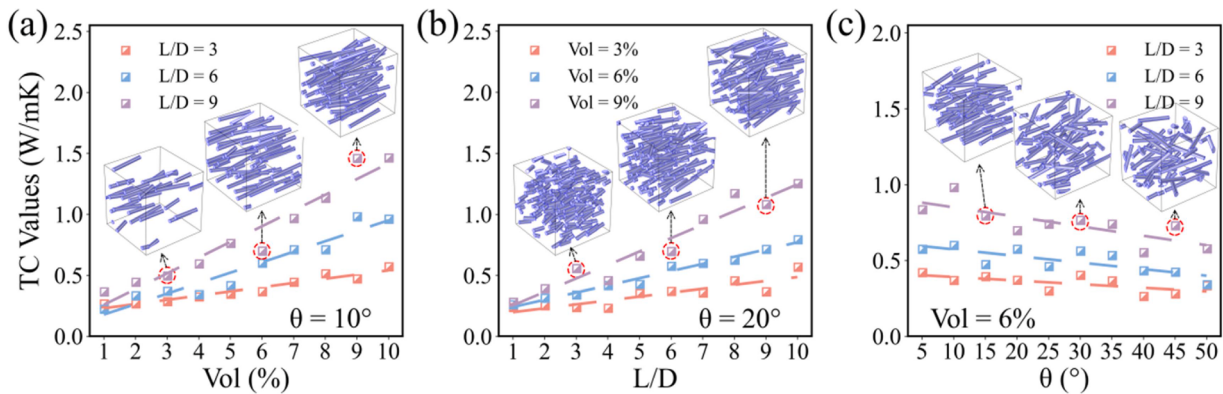


Fig. 9. Effects of different descriptors of carbon fibers on TC of composites. (a) Volume fraction. (b) Aspect ratio. (c) normally distributed angles.

As evidenced by Fig. 10(a), the CNN model nearly reaches its peak performance when the number of sections used reached 18, and further addition of images did not significantly enhance the model's performance. Therefore, in order to strike a balance between training costs and prediction accuracy, we selected a total of 18 sections perpendicular to the x-axis and z-axis as the datasets for training our model, which we designate as model_A. The loss function curves of this model on the training and test sets are depicted in Fig. 10(b), a smaller loss means that the true value is closer to the predicted value.

Subsequently, we trained another CNN model (model_B) using dataset_B which constructed by the external surfaces of the RVE model, and compared its evaluation metrics with those of model_A, as illustrated in Fig. 11(a). The training curves of Model_B is shown in Fig. 11(b). Due to the large number of data points, we also included corresponding Kernel Density Estimation (KDE) graphs when plotting scatter plots on the training and test set, as illustrated in Fig. 11(c-d). In these KDE graphs, deeper shades of blue indicate areas with a higher density of data points and lighter shades of brown indicate areas with a lower density of data points. This visualization approach not only provides a clear representation of data distribution but also highlights the areas of concentration within the datasets. The result reveals that Model_B achieved an R^2 score of 0.924 and an RMSE of 0.070 W/mK on the test set, whereas Model_A attained only an R^2 score of 0.874 and an RMSE of 0.091 W/mK on the same datasets. This indicates that using the external surfaces of the RVE model as the datasets allowed the CNN model to achieve higher accuracy with relatively fewer images. Therefore, the external surfaces of the RVE models contain more comprehensive geometric features, enabling the CNN model to more accurately identify the true three-dimensional structure of the material. In contrast, employing internal cross-sections as the datasets not only increased the training costs of the CNN model but also resulted in comparatively lower accuracy. This is different from composite materials with randomly distributed fillers, for which a CNN model trained with fewer cross sections can have relatively high accuracy [32].

3.3. Prediction of TC based on the combination of deep learning and ensemble learning

While the deep learning algorithm CNN have already proven their precision in predicting the TC of materials, there still exists a limitation when dealing with different fillers and matrices. Multiple CNN models are necessary to be trained for accurately predicting the TC of composites consist of different filler-matrix combinations, which would

result in significant computational costs. However, if we use CNN solely to capture the geometric structure and use it as a descriptor for ensemble learning algorithms (such as RFR) for training, it will significantly reduce the cost associated with model development, and improve model generalization and accuracy.

For the polymer composites with oriented 1D fillers, their geometric characteristics are mainly the degree of orientation of the filler arrangement. Although we used the mean angle θ from a normal distribution to control the orientation of carbon fibers in the RVE models during the modeling process, the randomness of the normal distribution is quite significant. Additionally, in real-world scenarios, the angle distribution of carbon fibers is likely not to follow a normal distribution. Therefore, this parameter may not be suitable for accurately describing the orientation of carbon fibers. To quantitatively describe the distribution of carbon fibers, we introduced a new variable called 'Orientation Degree' (O_d), defined as follows:

$$O_d = \sqrt{\frac{1}{N} \sum_{i=1}^N \left(1 - \frac{|\theta_i|}{90^\circ}\right)^2} \quad (11)$$

where N is the number of carbon fiber in the RVE model, θ_i is the angle between the i th carbon fiber and the x-axis.

As can be inferred from Eq. (11), O_d measures the extent to which carbon fibers deviate from the x-axis. Its value ranges from 0 to 1, where a value of 1 indicates that the carbon fibers are perfectly aligned with the x-axis, while a value of 0 means that the carbon fibers are entirely distributed within the plane parallel to the y-z plane. Therefore, a smaller value of O_d indicates a greater deviation of the carbon fibers from the x-axis, resulting in less concentrated heat transfer along the x-axis. This negatively impacts the TC of the composite material in the x-axis direction.

We plotted the relationship between the orientation degree of carbon fibers and the TC of composite materials at different aspect ratios and volume fractions, as shown in Fig. 12. Due to the inherent randomness in the distribution of data points, we used curve fitting to reveal the underlying patterns among the data. From Fig. 12 (a-b), it can be observed that there is a clear linear relationship between O_d and the TC of the composite material. Specifically, changes in O_d can effectively predict changes in the composite's TC.

Although O_d has been proven to be a good machine learning descriptor, in practical scenarios, accurately measuring each carbon fiber's angle in three-dimensional space through experimental methods is challenging, especially when dealing with a large number of fibers. Such

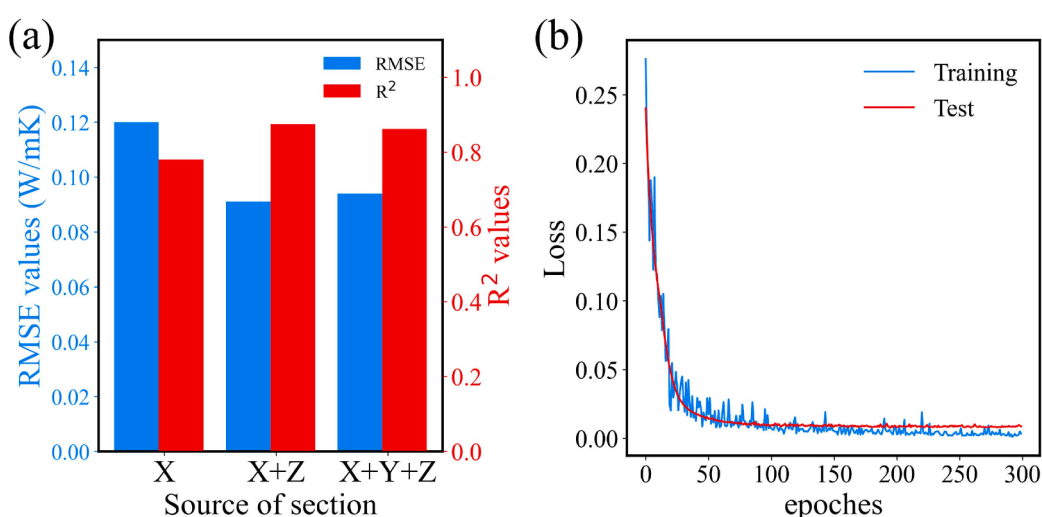


Fig. 10. (a) The effect of the number of sections on the performance of CNN model. (b) The learning curves of model_A (Using the cross-sections within the RVE model as input data) on the training and test sets.

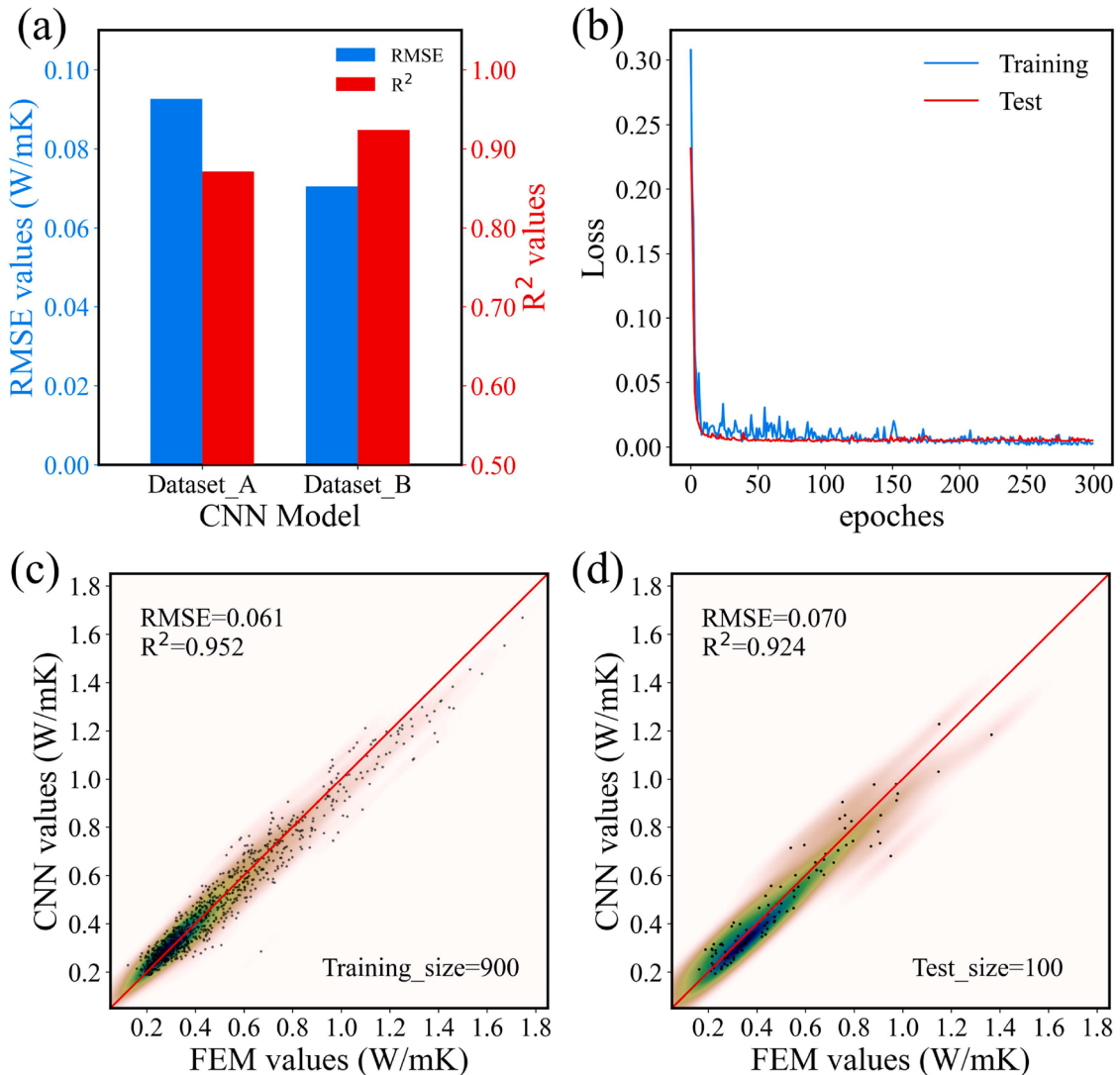


Fig. 11. (a) Comparison of evaluation metrics of Model_A (Using the cross-sections within the RVE model as input data) and Model_B (Using the external surfaces of the RVE model as input data) in the test set. (b) The learning curve of model_B. The prediction effect of model_B in the (c) training and (d) test sets.

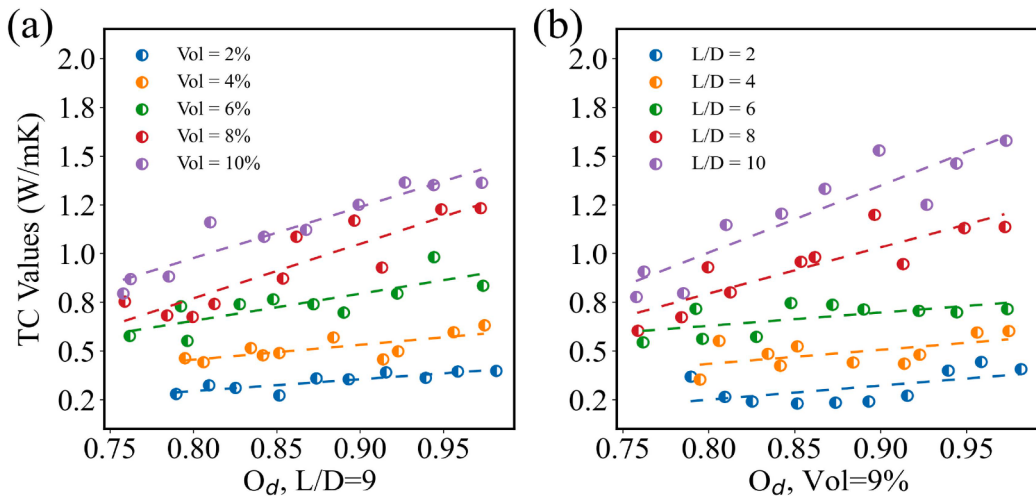


Fig. 12. The variation in TC of composites with the orientation degree of carbon fibers under different aspect ratios and volume fractions (a) $D/L = 9$. (b) $Vol=9\%$.

measurements, even if feasible, would incur significant time costs. For the other datasets that are obtained from the simulated RVE model, if the orientation information is not preserved during the model construction, it is also difficult to obtain the O_d data. Therefore, finding a method to quickly and easily obtain data on the angles of carbon fibers is crucial.

The CNN, with its inherent depth and unique convolutional kernel structure, is adept at precisely capturing geometric features in images. Therefore, we have employed CNN to predict the Orientation Degree of carbon fibers. We trained two separate models using the dataset of cross-sections (dataset_A) and external surfaces (dataset_B) of the RVE models, designated as model_C and model_D, respectively. The comparison of these two models on the test set, based on R^2 and RMSE metrics, is showcased in Fig. 13(a). The training curve of model_C is exhibited in Fig. 13(b), and the model's predictive performance on the training and test sets is respectively illustrated in Fig. 13 (c-d). The results reveal that model_D surpasses model_C in both RMSE and R^2 metrics, achieving 0.015 and 0.950 respectively on the test set, while model_C recorded 0.035 and 0.733. This indicates that CNN model achieves higher accuracy when trained with dataset_B, reiterating the advantage of using the external surfaces of the RVE model as training data due to its richer informational content compared to a singular cross-section.

Next, we utilized the RFR algorithm for TC prediction purposes. We employed Vol and D/L from Table 1 as features, and also incorporated the O_d mentioned above. The first two features are known quantities,

while O_d is the predicted value for the RVE model using Model_D. The correlation heat map of these features and the TC of composites material is shown in Fig. 14(a). When representing the orientation of anisotropic materials, average angle is a commonly used parameter [54]. Therefore, we trained models using both the average angle θ_{mean} and O_d separately, and compared the results. As observed in Fig. 14(b), the model performance was slightly better when using the O_d as a feature compared to using θ_{mean} , indicating that the orientation degree is more suitable as a descriptor for machine learning algorithms. Moreover, the prediction results of the RFR model using orientation degree as a feature for both the training and test sets are depicted in Fig. 14 (c-d). The model achieved RMSE values of 0.046 and 0.066, and R^2 scores of 0.971 and 0.954 on the training and test sets, respectively.

The prediction results indicate that when appropriate angular parameters are defined as features, traditional machine learning methods, such as the RFR model, can achieve higher accuracy than CNN model. Additionally, compared to CNN, RFR offers faster training speeds and lower training costs, on a computer with an AMD EPYC 9654 CPU and an NVIDIA L40 GPU, training a CNN takes approximately 1 h, whereas training a random forest takes only 1 min, presenting an efficient and rapid approach to estimate the TC of composite materials.

3.4. Prediction of TC of composites with different 1D fillers and matrixes

To further verify the strategy effectiveness of combining deep

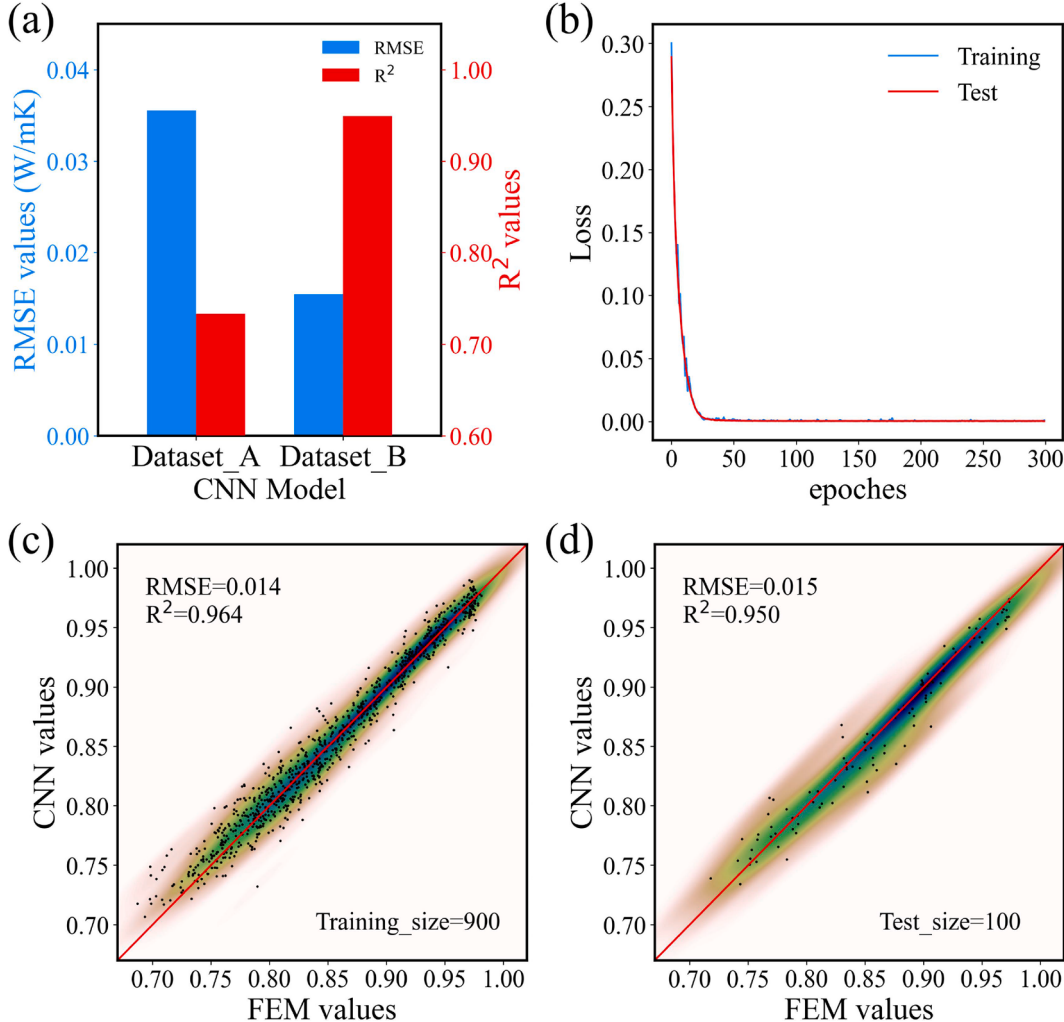


Fig. 13. (a) Comparison of evaluation metrics of Model_C (Using the cross-sections within the RVE model as input data) and Model_D (Using the external surfaces of the RVE model as input data) in the test set. (b) The learning curve of model_D. The prediction effect of model_D in the (c) training and (d) test sets.

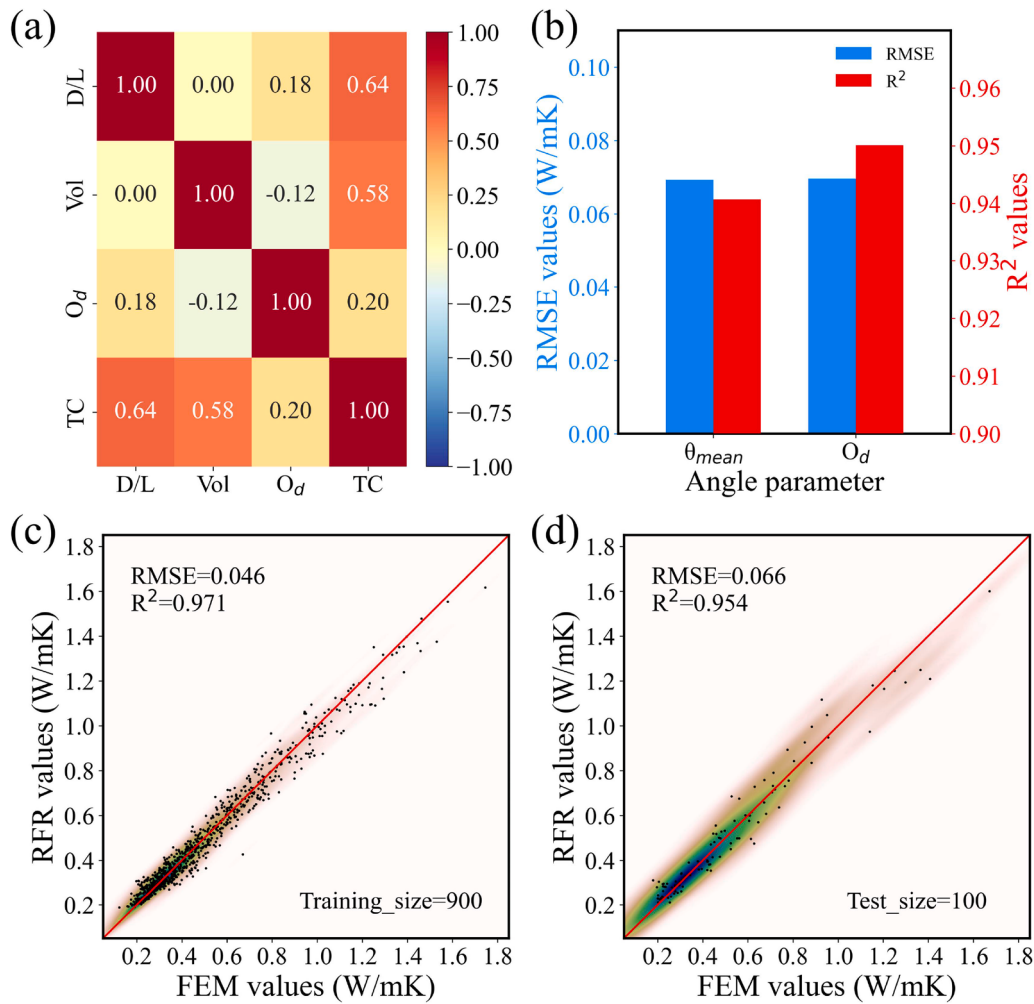


Fig. 14. (a) Heatmap of the correlations between different features and the TC of the composite material. (b) Comparison of the evaluation metrics on the test set for the RFR model using different angle parameters as features. The prediction effect of RFR in the (c) training and (d) test sets.

Table 2
Parameters of modeling.

Parameters	Range	Uniform Distribution Interval
TC _f (W/mK)	100–500	100
TC _m (W/mK)	0.1–0.5	0.1
Vol (%)	2–10	2

learning and ensemble learning, we extend this strategy to polymer composites with different 1D fillers and matrixes. We established a new RVE database based on the parameters shown in Table 2, with each RVE model, the angles θ of the 1D fibers are randomly generated within the range of 5° to 50°. The diameter of the fibers is fixed at 1.5 μm , and the aspect ratio is fixed at 10. The correlation heatmap between various descriptors is shown in Fig. 15(a), while the ranking of the correlation between the descriptors and the TC of the composite materials is illustrated in Fig. 15(b). The correlation among the selected descriptors is weak, while the correlation between the descriptors and the TC of the composites is strong.

During training, we divided the dataset into training and test sets with an 8:2 ratio and employed the TPE optimization algorithm to optimize the hyperparameters. The trained CNN model, model_D, is utilized to predict O_d based on the input of the external surfaces. Subsequently, using the predicted O_d along with descriptors such as volume fraction (Vol), matrix thermal conductivity (TC_m), and filler thermal conductivity (TC_f), a RFR algorithm is employed to estimate the TC of

composites. As shown in Fig. 15(c), the final RFR model achieved R² values of 0.995 and 0.960 on the training and test sets, respectively. Such high model accuracy proves the success of the above strategy.

To quantitatively describe the relationship between various descriptors and the TC of composite materials, we used SR to obtain mathematical expressions. We then compared the SR model's predictions with those from a traditional machine learning algorithm, RFR. To avoid overfitting, we employed the Tree-structured Parzen Estimator (TPE) optimization algorithm to tune the hyperparameters of the SR model. The SR models' predictions on the training and testing sets are shown in Fig. 15(d), with the mathematical expression provided in Eq. (12). The prediction results indicate that the SR model achieved almost the same level of accuracy as the RFR model, with the SR model even slightly outperforming the RFR on the test set, achieving an R² value of 0.976. Additionally, the SR model offers a clear mathematical expression, making it more interpretable than traditional machine learning models. This interpretability allows us to easily understand the relationships between various descriptors and the TC of the composite materials. Although the SR model's expression may not be highly precise due to the limited data available, we believe that as the dataset grows, the reliability of the expressions obtained by the SR model will increase significantly.

$$TC = TC_m + \frac{TC_m}{TC_f^2} + \frac{(0.805TC_f - 0.536) \times Vol}{\left(\frac{Vol \cdot O_d^2 + 2O_d \cdot Vol}{O_d/TC_m} + \frac{0.956Vol + TC_m}{0.284TC_f} \right)} \quad (12)$$

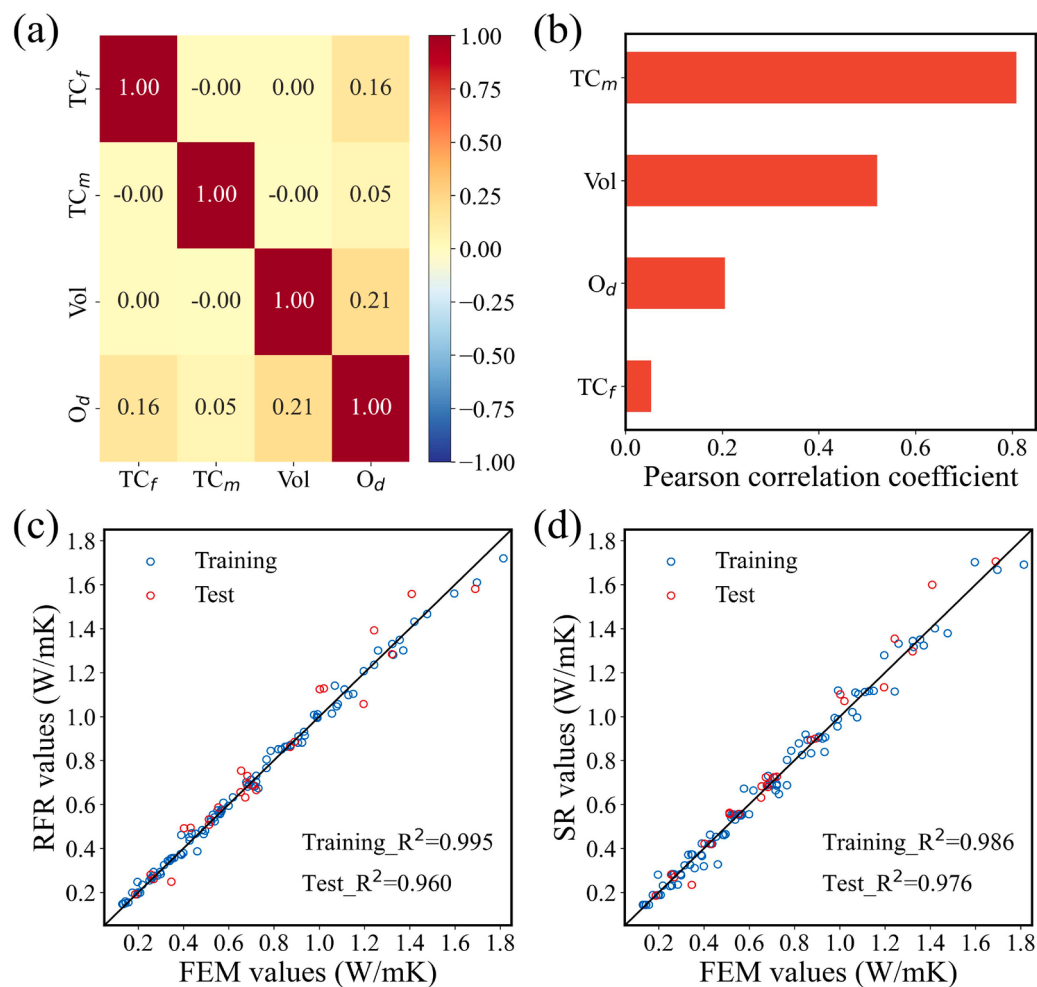


Fig. 15. (a) Heatmap of correlations between descriptors. (b) Ranking chart of the correlations between different descriptors and the TC of composites. Performance of (c) RFR and (d) SR models on training and test sets.

4. Conclusion

In this paper, we utilized CNN model to predict the TC of composite materials with 1D oriented carbon fiber filler. We constructed 1000 RVE models of composites and established two distinct datasets based on the internal cross-sections and external surfaces of these RVE models. The prediction results demonstrated that CNN models achieved higher performance when trained with the external surface as input, achieving an RMSE of 0.070 W/mK and an R^2 of 0.924 on the test set. This indicates that datasets composed of external surfaces contain richer information than those comprised of internal cross-sections. However, different CNN models need to be trained for composites composed of different matrices and fillers, resulting in wastes of computing resources. Therefore, we adopt the strategy of combining deep learning and ensemble learning to make full use of the advantages that deep learning can identify image features and ensemble learning has high accuracy and good generalization performance. Specifically, we defined a parameter termed 'orientation degree (O_d)' to quantitatively describe the distribution of carbon fibers in three-dimensional space. The deep learning algorithm CNN is used to predict O_d , achieving RMSE of 0.015 W/mK and R^2 of 0.950 on the test set. Then O_d was incorporated as a feature into the ensemble learning algorithm RFR for TC prediction. RMSE and R^2 of this model on the test set are 0.066 W/mK and 0.954 respectively, which is better than the CNN model for TC prediction. Subsequently, we successfully extended this strategy to composites consisting of different 1D oriented fillers and matrices, used the previously trained CNN model to

predict O_d , and trained the RFR model to predict TC, which greatly accelerated the model development. Furthermore, to quantitatively describe the relationship between O_d and TC of the composite material, we employed SR algorithm to obtain a mathematical expression of TC, which achieved an R^2 value of 0.976 on test sets. This strategy leverage CNN's inherent strength in understanding and interpreting complex geometry to streamline workflows and open the way for more scalable and cost-effective modeling solutions in materials science.

Declaration of competing interest

The authors declare that they have no known competing financial interests or personal relationships that could have appeared to influence the work reported in this paper.

Acknowledgements

This work was supported by the Natural Science Foundation of Shandong Province (Grant Nos. ZR2022QA092, ZR2022MA011, ZR2023QE223), the Excellent Young Scientists Fund (Overseas) of Shandong Province (Grant No. 2022HWYQ-091), and the Taishan Scholars Program of Shandong Province.

References

- [1] Cahill DG, Braun PV, Chen G, Clarke DR, Fan S, Goodson KE, Kebinski P, King WP, Mahan GD, Majumdar A, Maris HJ, Phillipot SR, Pop E, Shi L. Nanoscale thermal

- transport. II. 2003–2012. *Appl Phys Rev* 2014;1(1):011305. <https://doi.org/10.1063/1.4832615>.
- [2] Qian X, Zhou J, Chen G. Phonon-engineered extreme thermal conductivity materials. *Nat Mater* 2021;20(9):1188–202. <https://doi.org/10.1038/s41563-021-00918-3>.
- [3] Hansson J, Nilsson TMJ, Ye L, Liu J. Novel nanostructured thermal interface materials: a review. *Int Mater Rev* 2017;63(1):22–45. <https://doi.org/10.1080/09506608.2017.1301014>.
- [4] Hou J, Li G, Yang N, Qin L, Grami ME, Zhang Q, Wang N, Qu X. Preparation and characterization of surface modified boron nitride epoxy composites with enhanced thermal conductivity. *RSC Adv* 2014;4(83):44282–90. <https://doi.org/10.1039/c4ra07394k>.
- [5] Su J, Liu X, Charmchi M, Sun H. Experimental and numerical study of anisotropic thermal conductivity of magnetically aligned PDMS/Ni particle composites. *Int J Heat Mass Transfer* 2016;97:645–52. <https://doi.org/10.1016/j.ijheatmasstransfer.2016.02.023>.
- [6] Wan XH, Wang LG, Zuo B, Wang EZ, Zhu GZ. Studies on the thermal conductivity of Al₂O₃/Epoxy resin composite materials. *Adv Mater Res* 2012;535–537:235–8. <https://doi.org/10.4028/www.scientific.net/AMR.535-537.235>.
- [7] Puneet P, Rao AM, Podila R. Shape-controlled carbon nanotube architectures for thermal management in aerospace applications. *MRS Bull* 2015;40(10):850–5. <https://doi.org/10.1557/mrs.2015.229>.
- [8] Mainka H, Täger O, Körner E, Hilfert L, Busse S, Edelmann FT, Herrmann AS. Lignin – an alternative precursor for sustainable and cost-effective automotive carbon fiber. *J Mater Res Technol* 2015;4(3):283–96. <https://doi.org/10.1016/j.jmrt.2015.03.004>.
- [9] Ma J, Shang T, Ren L, Yao Y, Zhang T, Xie J, Zhang B, Zeng X, Sun R, Xu JB, Wong CP. Through-plane assembly of carbon fibers into 3D skeleton achieving enhanced thermal conductivity of a thermal interface material. *Chem Eng J* 2020; 380:122550. <https://doi.org/10.1016/j.cej.2019.122550>.
- [10] Hu X, Huang M, Kong N, Han F, Tan R, Huang Q. Enhancing the electrical insulation of highly thermally conductive carbon fiber powders by SiC ceramic coating for efficient thermal interface materials. *Composites, Part B* 2021;227: 109398. <https://doi.org/10.1016/j.compositesb.2021.109398>.
- [11] Shi Z, Zhang C, Chen XG, Li A, Zhang YF. Thermal, mechanical and electrical properties of carbon fiber fabric and graphene reinforced segmented polyurethane composites. *Nanomaterials* 2021;11(5):1289. <https://doi.org/10.3390/nano11051289>.
- [12] Li J, Ye Z, Mo P, Pang Y, Gao E, Zhang C, Du G, Sun R, Zeng X. Compliance-tunable thermal interface materials based on vertically oriented carbon fiber arrays for high-performance thermal management. *Compos Sci Technol* 2023;234:109948. <https://doi.org/10.1016/j.compscitech.2023.109948>.
- [13] Huang R, Ding D, Guo X, Liu C, Li X, Jiang G, Zhang Y, Chen Y, Cai W, Zhang Xa. Improving through-plane thermal conductivity of PDMS-based composites using highly oriented carbon fibers bridged by Al2O3 particles. *Compos Sci Technol* 2022;230:109717. <https://doi.org/10.1016/j.compscitech.2022.109717>.
- [14] Ding D, Huang R, Wang X, Zhang S, Wu Y, Zhang Xa, Qin G, Liu Z, Zhang Q, Chen Y. Thermally conductive silicone rubber composites with vertically oriented carbon fibers: a new perspective on the heat conduction mechanism. *Chem Eng J* 2022;441:136104. <https://doi.org/10.1016/j.cej.2022.136104>.
- [15] Chen H, Ginzburg VV, Yang J, Yang Y, Liu W, Huang Y, Du L, Chen B. Thermal conductivity of polymer-based composites: fundamentals and applications. *Prog Polym Sci* 2016;59:41–85. <https://doi.org/10.1016/j.progpolymsci.2016.03.001>.
- [16] Guo Y, Ruan K, Shi X, Yang X, Gu J. Factors affecting thermal conductivities of the polymers and polymer composites: a review. *Compos Sci Technol* 2020;193: 108134. <https://doi.org/10.1016/j.compscitech.2020.108134>.
- [17] Nan CW, Birringer R, Clarke DR, Gleiter H. Effective thermal conductivity of particulate composites with interfacial thermal resistance. *J Appl Phys* 1997;81(10):6692–9. <https://doi.org/10.1063/1.365209>.
- [18] Fu SY, Mai YW. Thermal conductivity of misaligned short-fiber-reinforced polymer composites. *J Appl Polym Sci* 2003;88(6):1497–505. <https://doi.org/10.1002/app.11864>.
- [19] Yang X, Wu H, Liu C, Zhang X. A novel analytic model for prediction of the anisotropic thermal conductivity in polymer composites containing aligned 1D nanofillers. *Int J Therm Sci* 2023;184:107980. <https://doi.org/10.1016/j.ijthermalsci.2022.107980>.
- [20] Klett JW, Ervin VJ, Edie DD. Finite-element modeling of heat transfer in carbon/carbon composites. *Compos Sci Technol* 1999;59:593–607. [https://doi.org/10.1016/s0266-3538\(98\)00099-2](https://doi.org/10.1016/s0266-3538(98)00099-2).
- [21] Pan Y, Iorga L, Pelegri AA. Numerical generation of a random chopped fiber composite RVE and its elastic properties. *Compos Sci Technol* 2008;68(13): 2792–8. <https://doi.org/10.1016/j.compscitech.2008.06.007>.
- [22] Liu B, Vu-Bac N, Zhuang X, Fu X, Rabczuk T. Stochastic full-range multiscale modeling of thermal conductivity of Polymeric carbon nanotubes composites: a machine learning approach. *Compos Struct* 2022;289:115393. <https://doi.org/10.1016/j.compstruct.2022.115393>.
- [23] Shokrieh MM, Rafiee R. Development of a full range multi-scale model to obtain elastic properties of CNT/polymer composites. *Iran. Polym J* 2012;21(6):397–402. <https://doi.org/10.1007/s13726-012-0043-0>.
- [24] Wei H, Bao H, Ruan X. Machine learning prediction of thermal transport in porous media with physics-based descriptors. *Int J Heat Mass Transfer* 2020;160:120176. <https://doi.org/10.1016/j.ijheatmasstransfer.2020.120176>.
- [25] Wan J, Jiang JW, Park HS. Machine learning-based design of porous graphene with low thermal conductivity. *Carbon N Y* 2020;157:262–9. <https://doi.org/10.1016/j.carbon.2019.10.037>.
- [26] Champa-Bujaico E, García-Díaz P, Díez-Pascual AM. Machine learning for property prediction and optimization of polymeric nanocomposites: a state-of-the-art. *Int J Mol Sci* 2022;23(18):10712. <https://doi.org/10.3390/ijms231810712>.
- [27] Hashemi MS, Safridi M, Sheidaei A. A supervised machine learning approach for accelerating the design of particulate composites: application to thermal conductivity. *Comput Mater Sci* 2021;197:110664. <https://doi.org/10.1016/j.commatsci.2021.110664>.
- [28] Fathidoost M, Yang Y, Oechsner M, Xu BX. Data-driven thermal and percolation analyses of 3D composite structures with interface resistance. *Mater Des* 2023;227: 111746. <https://doi.org/10.1016/j.matdes.2023.111746>.
- [29] Xu Y, Liu X, Cao X, Huang C, Liu E, Qian S, Liu X, Wu Y, Dong F, Qiu CW, Qiu J, Hua K, Su W, Wu J, Xu H, Han Y, Fu C, Yin Z, Liu M, Roepman R, Dietmann S, Virta M, Kangera F, Zhang Z, Zhang L, Zhao T, Dai J, Yang J, Lan L, Luo M, Liu Z, An T, Zhang B, He X, Cong S, Liu X, Zhang W, Lewis JP, Tiedje JM, Wang Q, An Z, Wang F, Zhang L, Huang T, Lu C, Cai Z, Wang F, Zhang J. Artificial intelligence: a powerful paradigm for scientific research. *The Innovation* 2021;2(4):100179. <https://doi.org/10.1016/j.xinn.2021.100179>.
- [30] Ma H, Jiao Y, Guo W, Liu X, Li Y, Wen X. Machine learning predicts atomistic structures of multilevel solid surfaces for heterogeneous catalysts in variable environments. *The Innovation* 2024;5(2):100571. <https://doi.org/10.1016/j.xinn.2024.100571>.
- [31] Wei H, Zhao S, Rong Q, Bao H. Predicting the effective thermal conductivities of composite materials and porous media by machine learning methods. *Int J Heat Mass Transfer* 2018;127:908–16. <https://doi.org/10.1016/j.ijheatmasstransfer.2018.08.082>.
- [32] Rong Q, Wei H, Huang X, Bao H. Predicting the effective thermal conductivity of composites from cross sections images using deep learning methods. *Compos Sci Technol* 2019;184:107861. <https://doi.org/10.1016/j.compscitech.2019.107861>.
- [33] Shen C, Sheng Q, Zhao H. Predicting effective thermal conductivity of fibrous and particulate composite materials using convolutional neural network. *Mech Mater* 2023;186:104804. <https://doi.org/10.1016/j.mechmat.2023.104804>.
- [34] Wu J, Song X, Gong Y, Yang W, Chen L, He S, Lin J, Bian X. Analysis of the heat conduction mechanism for Al2O3/Silicone rubber composite material with FEM based on experiment observations. *Compos Sci Technol* 2021;210:108809. <https://doi.org/10.1016/j.compscitech.2021.108809>.
- [35] He B, Mortazavi B, Zhuang X, Rabczuk T. Modeling Kapitza resistance of two-phase composite material. *Compos Struct* 2016;152:939–46. <https://doi.org/10.1016/j.composit.2016.06.025>.
- [36] Silani M, Talebi H, Ziae Rad S, Kerfriden P, Bordas SPA, Rabczuk T. Stochastic modelling of clay/epoxy nanocomposites. *Compos Struct* 2014;118:241–9. <https://doi.org/10.1016/j.compsctruct.2014.07.009>.
- [37] Liu B, Vu-Bac N, Rabczuk T. A stochastic multiscale method for the prediction of the thermal conductivity of Polymer nanocomposites through hybrid machine learning algorithms. *Compos Struct* 2021;273:114269. <https://doi.org/10.1016/j.compsctruct.2021.114269>.
- [38] Pan Y, Iorga L, Pelegri AA. Analysis of 3D random chopped fiber reinforced composites using FEM and random sequential adsorption. *Comput Mater Sci* 2008; 43(3):450–61. <https://doi.org/10.1016/j.commatsci.2007.12.016>.
- [39] Liu B, Vu-Bac N, Rabczuk T. Stochastic multiscale modeling of heat conductivity of Polymeric clay nanocomposites. *Mech Mater* 2020;142:103280. <https://doi.org/10.1016/j.mechmat.2019.103280>.
- [40] Chan YN, Huang SC, Li HT. Thermal conductivity of epoxy composites with controlled high loading of ceramic particles. *Japan Instit Electr Packag, ICEP-IAAC* 2015 Proceed 2015:258–61. <https://doi.org/10.1109/ICEP-IAAC.2015.7111034>.
- [41] Xu C, Sun Z, Shao G. Prediction of effective thermal conductivities of four-directional carbon/carbon composites by unit cells with different sizes. *Appl Sci* 2021;11(3):1171. <https://doi.org/10.3390/app11031171>.
- [42] Xiaoguang ZHANG, Baoku ZHANG, Yan H. Numerical simulation of thermal conductivity of rubber composite with randomly distributed carbon fibers. *Mater Reports* 2016;30(24):148–51. <https://doi.org/10.11896/j.issn.1005-023X.2016.24.028>.
- [43] Yang M, Li X, Yuan J, Wen Z, Kang G. A comprehensive study on the effective thermal conductivity of random hybrid polymer composites. *Int J Heat Mass Transfer* 2022;182:121936. <https://doi.org/10.1016/j.ijheatmasstransfer.2021.121936>.
- [44] Wang M, Pan N. Predictions of effective physical properties of complex multiphase materials. *Mater* 2008;63(1):1–30. <https://doi.org/10.1016/j.mser.2008.07.001>.
- [45] Zhou F, Cheng G. Lattice Boltzmann model for predicting effective thermal conductivity of composite with randomly distributed particles: considering effect of interactions between particles and matrix. *Comput Mater Sci* 2014;92:157–65. <https://doi.org/10.1016/j.commatsci.2014.05.039>.
- [46] Zhang H, Yu H, Meng S, Huang M, Micheal M, Su J, Liu H, Wu H. Fast and accurate reconstruction of large-scale 3D porous media using deep learning. *J Petrol Sci Eng* 2022;217:110937. <https://doi.org/10.1016/j.petrol.2022.110937>.
- [47] Sermanet P, LeCun Y. Traffic sign recognition with multi-scale convolutional networks. In: The 2011 International joint conference on neural networks; 2011. p. 2809–13. <https://doi.org/10.1109/IJCNN.2011.6033589>.
- [48] Ji S, Xu W, Yang M, Yu K. 3D Convolutional neural networks for human action recognition. *IEEE Trans Pattern Anal Mach Intell* 2013;35(1):221–31. <https://doi.org/10.1109/tpami.2012.59>.
- [49] Ioffe S, Szegedy C. Batch normalization: accelerating deep network training by reducing internal covariate shift. Cornell University Library; 2015. arXiv.org, Ithaca.
- [50] Srivastava N, Hinton G, Krizhevsky A, Sutskever I, Salakhutdinov R. Dropout: a simple way to prevent neural networks from overfitting. *J Mach Learn Res* 2014; 15:1929–58.

- [51] Muzny CD, Huber ML, Kazakov AF. Correlation for the viscosity of normal hydrogen obtained from symbolic regression. *J Chem Eng Data* 2013;58(4): 969–79. <https://doi.org/10.1021/je301273j>.
- [52] Mueller T, Hernandez A, Wang C. Machine learning for interatomic potential models. *J Chem Phys* 2020;152(5):050902. <https://doi.org/10.1063/1.5126336>.
- [53] Loftis C, Yuan K, Zhao Y, Hu M, Hu J. Lattice thermal conductivity prediction using symbolic regression and machine learning. *J Phys Chem A* 2020;125(1):435–50. <https://doi.org/10.1021/acs.jpca.0c08103>.
- [54] Hu Q, Bai X, Zhang C, Zeng X, Huang Z, Li J, Li J, Zhang Y. Oriented BN/Silicone rubber composite thermal interface materials with high out-of-plane thermal conductivity and flexibility. *Composit, Part A* 2022;152:106681. <https://doi.org/10.1016/j.compositesa.2021.106681>.